

Accuracy of the VLTI Optical Alignment

Stéphane Guisard*
European Southern Observatory, Paranal Observatory

ABSTRACT

Since mid 2002, the complete optical trains of the four 8m Unit Telescopes (UT) are installed and aligned to provide the Very Large Telescope Interferometer (VLTI) with a unique choice of beam combination possibilities [1]. A description of the optical alignment method used and of the final image quality has been given in [2]. We describe in this document the analytical approach used to quantify the geometrical alignment errors not only at the end of the optical train but also at each optical subsystem level.

Keywords: VLTI, Optical Alignment.

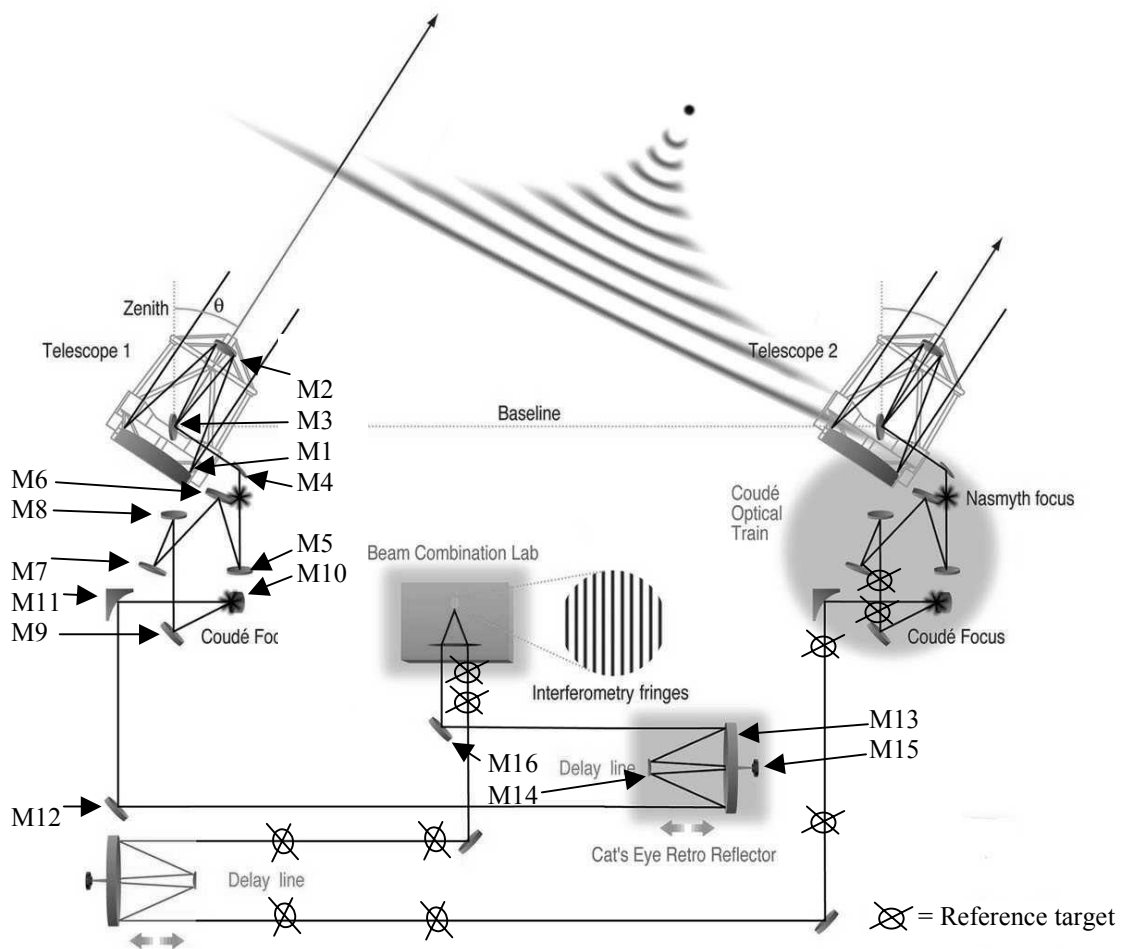


Figure1 : VLTI optical components location from M1 to M16

*
sguisard@eso.org, ESO, Alonso de Cordova 3107, Santiago, Chile

1. INTRODUCTION

The study presented in this document has been developed for the VLTI in the case of the UT. It includes the optical subsystems starting after the telescope relay optics, namely at M12 level, and ending just before the VLTI instrument. The included subsystems are therefore following the light path: the M12, the cat-eye (CE), the M16, the beam compressor (BC) and the switchyard mirror (SY). The main reason for starting after the relay optics, is that from there, it is always possible to bring the image and pupil aligned with the alignment references located in the light duct before the M12. This alignment is performed using telescope pointing and M10 movements (motorized mirror located in an image plane). The other reason is that the distances within the UT down to M11 mirror are relatively small compared to the distances after M11 (light ducts, VLTI tunnel). Small angular alignment errors along these distances turn into millimeters of displacement of the image or pupil.

In this study we use 1st order optics, an approximation that is fully justified by the amount of misalignment in play. The consequence is that all the misalignment effect can be combined linearly.

2. MATHEMATICAL APPROACH

2.1. Definition of the subsystems local coordinate systems

As explained in detail in [2], we defined an input axis and an output axis for each VLTI subsystem and each axis is materialized by pairs of distant removable crosshairs. For all the subsystems located after the M9, the input and output axis are located in horizontal planes (called incidence planes B and C in [2]). We define for these subsystems local input coordinate systems (O, X, Y, Z) and local output coordinate systems (O', X', Y', Z') so that (see figure 2):

- Y and Y' are vertical pointing upwards.
- Z and Z' are oriented in the direction of light and are passing by the lines defined by the reference crosshairs.
- (O, X, Y, Z) and (O', X', Y', Z') are normalized direct coordinate systems (implying that X and X' are horizontal pointing to the right when looking in the direction of light).
- the origins O and O' of the coordinates systems on the input and output axis are chosen at convenient positions depending on each subsystem.

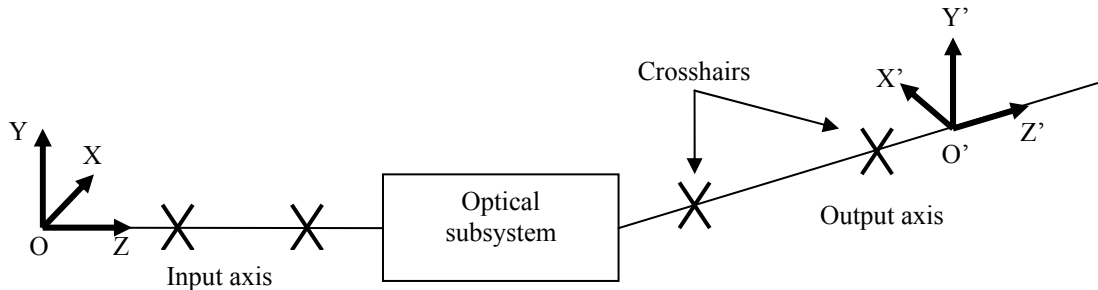


Figure 2: Local coordinate systems of an optical subsystem

2.2. Definition of the ray misalignment

Since we are interested in lateral beam misalignments, we can define a beam misalignment by 4 parameters : ΔX , ΔY , θX , θY referred to the coordinate system where the beam is. For an input beam, ΔX and ΔY are therefore the coordinates of the beam crossing with the plane (OXY) while θX (resp. θY) is the angular coordinate of the beam in the vertical (resp. horizontal) plane, measured from the beam towards the OZ axis and positively for a positive rotation around the OX (resp. OY) axis.

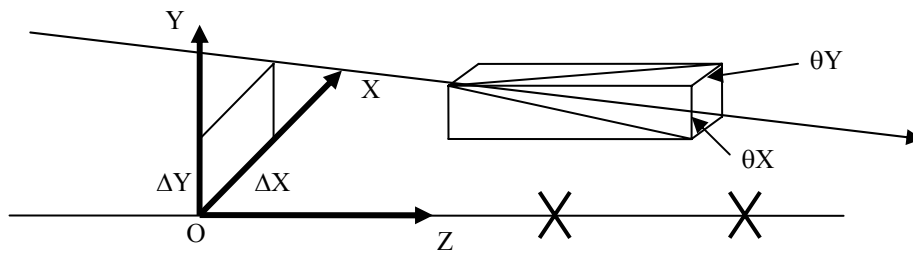


Figure 3: Ray misalignment components

2.3. The incident ray motion matrix

In a perfectly aligned system, a light beam entering exactly on the subsystem input axis will emerge exactly on the subsystem output axis. However, to a misaligned input beam defined by an error vector $[R] = (\Delta X, \Delta Y, \theta X, \theta Y)$ will correspond a misaligned output beam (see figure 4) defined by the error vector $[R'] = (\Delta X', \Delta Y', \theta X', \theta Y')$. Relation between $[R]$ and $[R']$ is done through what we call "the incident ray motion matrix" $[Mi]$ defined for each subsystem i . $[Mi]$ is a 4x4 matrix and we have, using matrix notation, the relation : $[R'i] = [Mi]x[Ri]$.

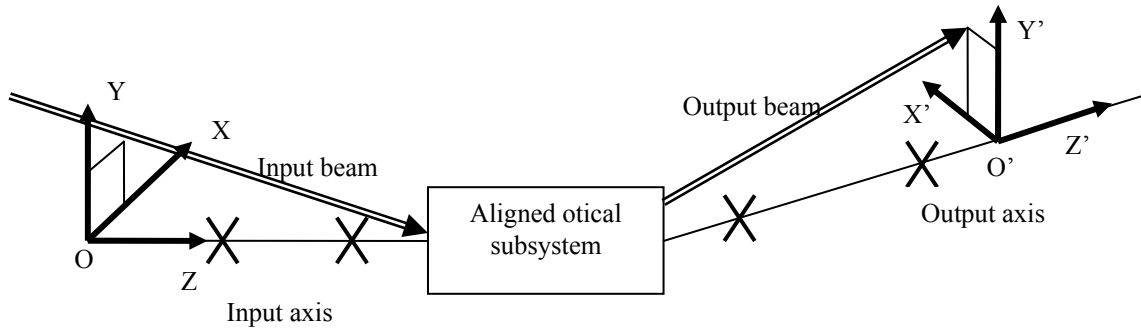


Figure 4: VLT optical components location from M1 to M16

2.4. The subsystem misalignment vector

The "subsystem misalignment vector" $[Ni]$ represents the effects of an internal static misalignment of the subsystem i on the direction and position of the output beam for a perfectly aligned input beam. This vector could be derived from calculations or specifications, but usually it is the result of direct measurements made during the internal alignment of the subsystem.

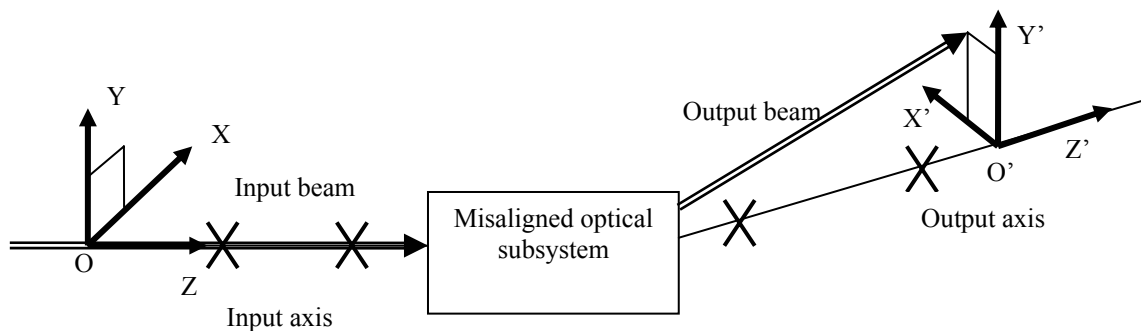


Figure 5: Effect of a misaligned optical subsystem on a perfectly aligned input beam

2.5. The subsystem motion matrix

The “subsystem motion matrix” $[O_i]$ is a 6 by 4 matrix that characterizes the effect of misplacement of the optical subsystem with respect to the input reference axis. This misplacement of the subsystem makes a perfectly aligned input beam to emerge misaligned with respect to the output reference axis (see figure 6). The misplacement of the subsystem i is defined by a “subsystem position error vector” $[S_i] = (\Delta X, \Delta Y, \Delta Z, \theta X, \theta Y, \theta Z)$. The definition of ΔZ and θZ is in line with the definition of the other linear and angular coordinates errors in X and Y. We express $[S_i]$ in the local input coordinate reference system. The resulting output beam position error is given by the matrix product $[O_i].[S_i]$. For static subsystems, this error is seen simply as a subsystem internal misalignment and is included in the matrix $[N_i]$ automatically. For moving subsystems however, like the cat-eyes on the delay line rails, motorized mirrors like M16 or switchyard mirrors, the two effects have to be separated, matrix $[N_i]$ containing the static alignment error and matrix $[O_i]$ containing the dynamic alignment error provoked by system motion.

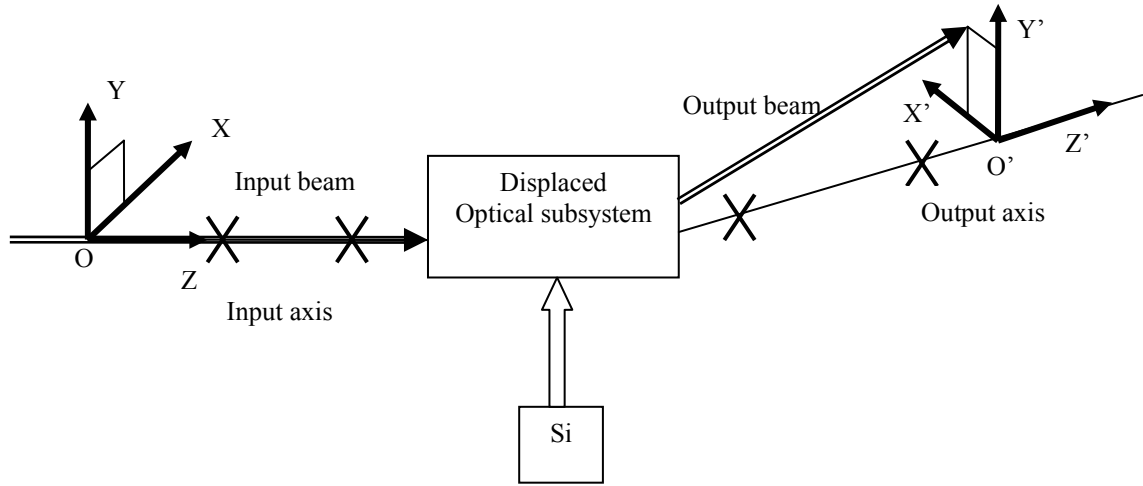


Figure 6: Effect of a displaced optical subsystem on a perfectly aligned input beam

2.6. The propagation matrix

Neglecting atmospheric effects which are beyond the scope of this study, propagation in free space of a beam does not change the direction errors of the beam but only its lateral positioning. At a distance d , defined positively along the local z direction of propagation, the initial positioning error vector $[R_o]$ ($\Delta X_o, \Delta Y_o, \theta X_o, \theta Y_o$) becomes a positioning error vector $[R_d]$ ($\Delta X_d, \Delta Y_d, \theta X_d, \theta Y_d$). Relations between $[R_o]$ and $[R_d]$ coordinates are given by :

$$\begin{aligned}\Delta X_d &= \Delta X_o + \theta Y_o \times d \\ \Delta Y_d &= \Delta Y_o - \theta X_o \times d \\ \theta X_d &= \theta X_o \\ \theta Y_d &= \theta Y_o\end{aligned}$$

In matrix notation we can define the propagation matrix $Q_i(d)$.

$$Q_i(d) = \begin{bmatrix} 1 & 0 & 0 & d \\ 0 & 1 & -d & 0 \\ 0 & 0 & 1 & 0 \\ 0 & 0 & 0 & 1 \end{bmatrix}$$

2.7. Combined effect

The relation between the misalignment vector $[R_i]$ at the entrance of the subsystem i and the corresponding vector $[R_{i+1}]$ at the entrance of the following subsystem $i+1$ is given by the linear combination of the different error matrices and vectors.

$$[R_{i+1}] = [Q_i] \times ([N_i] + [O_i] \times [S_i] + [M_i] \times [R_i])$$

3. STATISTICAL APPROACH

For this study we express the centering and angular errors in terms of standard deviation σ , assuming that errors have a Gaussian distribution. When we want to have a Peak to Valley (PV) error we will take the values at $\pm 3\sigma$, which in the case of a Gaussian distribution of the errors corresponds to 99.7% of the case.

When aligning we always bring these errors to "zero", however errors in measurements, adjustments and repositioning of the optics for example, statistically spread the error on a certain range. Depending on the cases, error sources are measured, calculated or estimated. Since most of the optical systems in the VLTI are multiples of 4 or 8, we make also the assumption of ergodicity when evaluating the error sources. It means we assume that statistically the errors made when adjusting the same system N times has the same statistical distribution as adjusting N identical systems once.

4. SUBSYSTEMS MATRICES

4.1. M12, M16 and switchyard mirrors.

M12, M16 and switchyard mirrors are flat mirrors inclined at 45 degrees around a vertical axis, bending the light 90 degrees. Two cases can be defined depending if the mirrors fold the light to the left or to the right when looking in the direction of light. We take the origins O and O' of the input and output coordinate systems at the intersection of the z and z' axis (they should by construction always cross each other), that is on the mirror surface.

For a flat mirror inclined 45 degrees and sending the light 90 degrees towards the left (resp right) the incident ray motion matrix $[M1L]$ (resp. $[M1R]$), and the mirror motion matrix $[O1L]$ (resp. $[O1R]$) are :

$$[M1L] = \begin{bmatrix} -1 & 0 & 0 & 0 \\ 0 & 1 & 0 & 0 \\ 0 & 0 & 1 & 0 \\ 0 & 0 & 0 & -1 \end{bmatrix} \quad [O1L] = \begin{bmatrix} 1 & 0 & -1 & 0 & 0 & 0 \\ 0 & 0 & 0 & 0 & 0 & 0 \\ 0 & 0 & 0 & -1 & 0 & -1 \\ 0 & 0 & 0 & 0 & 2 & 0 \end{bmatrix}$$

$$[M1R] = \begin{bmatrix} -1 & 0 & 0 & 0 \\ 0 & 1 & 0 & 0 \\ 0 & 0 & 1 & 0 \\ 0 & 0 & 0 & -1 \end{bmatrix} \quad [O1R] = \begin{bmatrix} 1 & 0 & 1 & 0 & 0 & 0 \\ 0 & 0 & 0 & 0 & 0 & 0 \\ 0 & 0 & 0 & -1 & 0 & 1 \\ 0 & 0 & 0 & 0 & 2 & 0 \end{bmatrix}$$

4.2. Cat-eye

Whatever the position of the cat-eye on the delay lines rails is, the cat-eye reimages the pupil of the VLTI onto itself with a magnification of 1. This is done by an appropriate setting of the curvature of its variable curvature mirror (VCM). We therefore choose the origins O and O' of our local coordinate systems for the cat's-eye at the VLTI pupil in the middle of the delay line tunnel.

Calling dp the distance from the VLTI pupil to the cat-eye primary mirror, the incident ray motion matrix $[Mce]$ and cat's-eye motion matrix $[Oce]$ are :

$$[Mce] = \begin{bmatrix} 1 & 0 & 0 & 0 \\ 0 & -1 & 0 & 0 \\ 0 & 0 & -1 & 0 \\ 0 & 0 & 0 & 1 \end{bmatrix} \quad [Oce] = \begin{bmatrix} -2 & 0 & 0 & 0 & 2dp & 0 \\ 0 & 2 & 0 & 2dp & 0 & 0 \\ 0 & 0 & 0 & 0 & 0 & 0 \\ 0 & 0 & 0 & 0 & 0 & 0 \end{bmatrix}$$

4.3. Beam Compressors

The beam compressors (BC) have a beam compression ratio of $Gybc = 18/80 = 0.225$. Their incident ray motion matrix $[Mbc]$ is given below. Origin O (resp. O') of entrance (resp. exit) reference system of the BC is taken at the local VLTI pupil before the BC (resp. after the BC).

$$[Mbc] = \begin{bmatrix} Gybc & 0 & 0 & 0 \\ 0 & -Gybc & 0 & 0 \\ 0 & 0 & -1/Gybc & 0 \\ 0 & 0 & 0 & 1/Gybc \end{bmatrix}$$

5. STUDY CASES

In the scope of this document we will limit our study to few cases only. For example in terms of distances only the beam combinations which are relevant in terms of change of distances will be treated. Indeed the distance between M12 and the tunnel center can vary a lot, as well as the distance of the cat-eye to the intermediate pupil at the center of the tunnel. For the other distances (M16 to beam compressor or beam compressor to switch-yard for example), it is sufficient to take an average value.

Our formalism enables the calculation of the beam positioning error anywhere along the light path. For the practical cases we usually calculate it at intermediate or final pupil position, this is why we choose most of our origin O and O' of local subsystems at intermediate VLTI pupil locations. As far as vigneting by mechanical and optical components is concerned, it is easy, from these intermediate pupil positions, to propagate or back-propagate the beam (using the propagation matrix) to the place we want and check for vigneting or tolerancing.

Following the study presented in this document we use the indices $i=1$ to 5 respectively for M12 / Cat-eye / M16 / Beam Compressor and Switch-yard and the following distances (see table 1) :

System index i	System name	Distance	Value (in mm)
1	M12	d1	69000
2	Cat-eye	Dp	66000
		d2	0
3	M16	d3	0
4	Beam Compressor	d4	-6500
5	Switch-yard	d5	6500

Table 1: system indices and names and distances used for the calculations

Some remarks :

- The beam arrives perfectly aligned on M12 (always possible by changing telescope pointing and M10 position).
- The distance between M12 and tunnel center is taken at its maximum value $d1=69000$ mm (worst case as for the misalignment effects).
- Because we assume M16 is located on the VLTI pupil re-imaged by the cat's-eye we have $d2=0$ (true for our purpose).
- The beam compressor takes the pupil image located on M16, it implies that $d3=0$. The Switch-yard mirror is located 6500 mm from the final pupil position, it implies that $d4=-6500$ mm (the beam will be "back-propagated" for the

calculation) and that $d_5=+6500$ mm.

6. CALCULATIONS

6.1. Introduction

In all the calculations that follow the errors are errors measured at each subsystem level during optical alignment. They are then recalculated at the final pupil position in the VLTI laboratory as if they were propagating through perfectly aligned downstream subsystems. Errors are expressed in arcsec on sky for beam direction errors and in percentage of the pupil diameter for the pupil lateral position error. We give the results in the worst case, that is for the largest distance from the tunnel center for both the M12 and the cat-eye. We distinguish 3 cases for the calculations as described in the next 3 paragraphs. The tables give the individual contribution (standard deviation values) of each subsystem from which a total standard deviation value is calculated. This approach is justified by the alignment approach used in the VLTI and detailed in [2], which makes the alignment of each subsystem independent from each other. This method might not give final alignment results as good as simply propagating a beam from one end of VLTI to the other and correcting pupil and image position in the VLTI laboratory (although we still do that when “zeroing” the error with telescope pointing and M10 offsets as explained in the next paragraphs). But it gives the VLTI great flexibility and extremely large choice of beam combinations and possible light paths, and will ensure minimum alignment error for any of these combinations, not only a fixed one (same telescope always feeding only the same cat’s eye, itself always only feeding the same beam compressor, etc ...). Finally the more important value at $\pm 3 \sigma$ corresponding to the semi amplitude of the global error is given in the last row.

6.2. Static case

What we call “static case” regroups the alignment errors (see table 2) left in the system after an alignment of the system, not including repositioning of the moving mirrors (like after a change of beam combination) nor the movement of cat-eyes during observation. Theoretically, these errors can be zeroed by a proper adjustment of the M10 image mirror and telescope pointing offsets. It is nevertheless important to quantify these errors for vignetting check and ensure that after this adjustment all the subsystems work in their designed working range.

System	Error at final pupil location (VLTI lab)			
	$\Delta X'$	$\Delta Y'$	$\theta X'$	$\theta Y'$
M12	1.02 %	0.72%	0.028 ″	0.040 ″
CE	0.50 %	0.50 %	0.001 ″	0.001 ″
M16	0.35 %	0.00 %	0.028 ″	0.040 ″
BC	1.11 %	1.11 %	0.011 ″	0.011 ″
SY	0.87 %	0.35 %	0.006 ″	0.009 ″
Total : σ	1.84 %	1.46 %	0.042 ″	0.058 ″
Total : $\frac{1}{2} PV$	$\pm 5.53 \%$	$\pm 4.37 \%$	$\pm 0.125 \text{ ″}$	$\pm 0.175 \text{ ″}$

Table 2 : individual and global error contributions of the subsystems in the “static case”

6.3. Repositioning case

The repositioning case regroups all the errors that can appear after a change of beam combination (see table 3).

System	Error at final pupil location (VLTI lab)			
	$\Delta X'$	$\Delta Y'$	$\theta X'$	$\theta Y'$
M12	0.34 %	0.24 %	0.009 ″	0.013 ″
CE	0.00 %	0.00 %	0.000 ″	0.000 ″
M16	0.01 %	0.00 %	0.017 ″	0.024 ″
BC	0.00 %	0.00 %	0.000 ″	0.000 ″
SY	2.52 %	0.00 %	0.032 ″	0.000 ″
Total : σ	2.54 %	0.24 %	0.037 ″	0.013 ″
Total : $\frac{1}{2} PV$	$\pm 7.62 \%$	$\pm 0.72 \%$	$\pm 0.112 \text{ ″}$	$\pm 0.030 \text{ ″}$

Table 3: individual and global error contributions of the subsystems in the “repositioning case”

These changes normally require a repositioning of the M12, M16 and switch-yard mirrors. The resulting errors, as for the static case, can also be zeroed, at the beginning of the observations, by applying further relative offsets to the M10 mirror and to the pointing of the telescope compared to the positions defined by the static alignment. We could consider the repositioning case as a “semi-static” mode (or “semi-dynamic”).

Due to a problem in some of the switch-yard motorized units, the repositioning of the SY mirror is not yet in specifications, leading to high error values for repositioning. The expected values when the problem will be solved are more likely to be according to table 4.

System	Error at final pupil location (VLTI lab)			
	$\Delta X'$	$\Delta Y'$	$\theta X'$	$\theta Y'$
M12	0.34 %	0.24 %	0.009 ″	0.013 ″
CE	0.00 %	0.00 %	0.000 ″	0.000 ″
M16	0.01 %	0.00 %	0.017 ″	0.024 ″
BC	0.00 %	0.00 %	0.000 ″	0.000 ″
SY	0.28 %	0.00 %	0.004 ″	0.000 ″
Total : σ	0.44 %	0.24 %	0.019 ″	0.013 ″
Total : $\frac{1}{2}$ PV	± 1.32 %	± 0.72 %	± 0.059 ″	± 0.030 ″

Table 4: individual and global error contribution of the subsystems in the expected “repositioning case”

6.4. Dynamic case (observation)

This case regroups the errors appearing during the observations, and after having zeroed the errors due to repositioning. They are therefore the errors that will appear during the observation assuming that no active pupil motion correction or telescope pointing offsets are done during observations. In practice they correspond only to the errors in cat-eye motion since this is the only active moving element during a given observation. Cat-eye motion accuracy is directly related to rail alignment. More precisely, we can show that pupil positioning is affected by the local tilt of the cat-eye carriage. Since we are still in a stage of installing new delay lines and constantly refining their alignment and trying to follow their stability, we have summarized, in table 5, 3 cases of rail alignment accuracy and derived the final beam positioning errors.

Rail alignment accuracy (Peak-Valley) Vertical and Horizontal	$\frac{1}{2}$ PV Errors at final pupil location (VLTI lab)			
	$\Delta X'$	$\Delta Y'$	$\theta X'$	$\theta Y'$
$\pm 1''$ (eq to ± 5 microns on rails)	± 0.80 %	± 0.80 %	± 0.000 ″	± 0.000 ″
$\pm 5''$ (eq to ± 25 microns on rails)	± 4.00 %	± 4.00 %	± 0.000 ″	± 0.000 ″
$\pm 10''$ (eq to ± 50 microns on rails)	± 8.00 %	± 8.00 %	± 0.000 ″	± 0.000 ″

Table 5 : Errors caused by cat-eye motion for 3 different rail alignment accuracy

At the time of writing, the accuracy of rail alignment is more likely somewhere between the last two cases for all the delay lines. Our goal is to get as close as possible to the first case. Rail systems were sufficiently well designed so that these values are reachable with a bit of care. The next interesting step will be to follow the stability of the alignment in time especially in a region where earthquakes are frequent.

7. CONCLUSIONS

The simple analytical approach developed in this document enables to derive easily alignment errors for the different optical subsystems composing the VLTI. Static errors remaining after alignment of the complete system remains well in the range of correction of the system (pupil and image displacements). Relocations of optics after a change of beam combination configuration are not yet as good as expected due to a temporary problem, although the errors resulting can be easily corrected as well. As for the motion of pupil during observations because of related cat’s-eye displacement on the delay lines, it is not yet as good as we would like and are working more carefully on the alignment of the rails.

8. REFERENCES

- [1] See for example ESO press release: <http://www.eso.org/outreach/press-rel/pr-2002/pr-16-02.html>
- [2] Optical alignment of the VLTI, S.Guisard, SPIE 2002, vol [4838-51].